Spatial Leggett-Garg inequalities

Guillem Müller-Rigat,[1] Donato Farina,[2] Maciej Lewenstein,[1,3] and Andrea Tononi[1,4]
[1]*ICFO-Institut de Ciencies Fotoniques, The Barcelona Institute of Science and Technology, Castelldefels, 08860 Barcelona, Spain*
[2]*Physics Department E. Pancini, Università degli Studi di Napoli Federico II, Complesso Universitario Monte S. Angelo, I-80126 Napoli, Italy*
[3]*ICREA, Pg. Lluís Companys 23, 08010 Barcelona, Spain*
[4]*Department de Física, Universitat Politècnica de Catalunya, Campus Nord B4-B5, E-08034 Barcelona, Spain*

(Received 31 October 2025; revised 23 March 2026; accepted 4 August 2026; published 20 August 2026)

We formulate a spatial extension of the Leggett-Garg inequality by considering three distant observers locally measuring a many-body system at three subsequent times. The spatial form is especially suitable to test the ability of quantum devices to generate spatiotemporal correlations in a Hamiltonian-agnostic manner. We illustrate our proposal for a Heisenberg chain in a magnetic field, showing indeed that the first inequality-violation time scales proportionally to the distance between measuring parties. We attribute this phenomenon to Lieb-Robinson physics and, confirming this connection, we find that violations are anticipated when increasing the interaction range. The inequality violation is readily observable in current quantum simulation platforms, particularly Rydberg atoms' arrays and ultracold atoms in optical lattices. In outlook, spatial Leggett-Garg inequalities constitute a practical tool for benchmarking the complex nonrelativistic dynamics of many-body quantum systems.

DOI: 10.1103/k8g5-crbz

I. INTRODUCTION

The Leggett-Garg inequality (LGI) [1] provides a testable criterion to analyze the correlations in time of an evolving physical system. Its formulation assumes intuitive classical concepts, like macroscopic realism, noninvasive measurability and induction [2,3], yielding constraints on the statistics of observations at multiple times. The first Leggett-Garg inequality violation by quantum systems was observed experimentally in 2010 [4]. This evidence, together with a long series of subsequent experiments [5–21] (see also the reviews [2,3]), requires us to adopt quantum mechanics as the everyday working tool for correctly describing correlations in microscopic systems.

In the past decades, Leggett-Garg inequalities have been extended to various scenarios, including multiple measurements and times [2,22,23], macroscopic spin-j systems (with j large) [24], and neutrino oscillations [10,25,26], and its loopholes [27,28] and limitations [29,30] have been addressed. In spin chains, extended Leggett-Garg inequalities based on repeated local or collective measurements have been proposed to witness equilibrium phase transitions [31,32] and as a quantum coherence witness [16]. Spatial versions, however, in which observers at different locations measure distinct parts of a time-evolving many-body system, have never been proposed. Such an extension could enable the analysis and certification of nonequilibrium features of many-body dynamics, including the light cone spreading of correlations [33–35].

In this paper, we introduce a spatial Leggett-Garg inequality for a protocol in which multiple parties perform spatially separated sequential measurements (see Fig. 1). In general, and in contrast with the standard Leggett-Garg inequality, the violation of the spatial Leggett-Garg inequality requires an interacting Hamiltonian. This feature allows its use as a figure of merit to benchmark the ability of a quantum system to generate spatiotemporal correlations in a system-agnostic way.

In principle, our conceptual extension is applicable to physical systems in any dimension and governed by arbitrary Hamiltonians. However, to illustrate the concepts in an experimentally relevant setting, we analyze the Leggett-Garg correlator for a (spatiotemporally) symmetric measurement protocol performed on a spin chain evolving under the Heisenberg Hamiltonian in a magnetic field [36,37]. We observe the reduction of the Leggett-Garg inequality violation when increasing the system size, showing that the propagation of a quantum signal through the chain is increasingly difficult for larger distances. Along this line, since time is necessary to establish correlations, the first instance of violation takes place at times increasing with the system size. This behavior is coherent with the fact that quantum correlations can be distributed in spin chains with finite velocity [34], theoretically limited by the Lieb-Robinson bound [38], that we can practically estimate. Furthermore, we show through our method that, compared to other models with similar Lieb-Robinson velocities, the maximal violation of the spatial Leggett-Garg inequality is actually achieved by the Heisenberg Hamiltonian. This result provides a method to certify its realization in quantum devices in an implementation-agnostic manner.

A further practical purpose of our work is providing a concrete proposal for the experimental observation of spatial Leggett-Garg inequality violations in spin chains. Suitable platforms are, e.g., Rydberg atoms [39–42], trapped atoms [43–45], ions [46,47], and ultracold atoms [48,49].

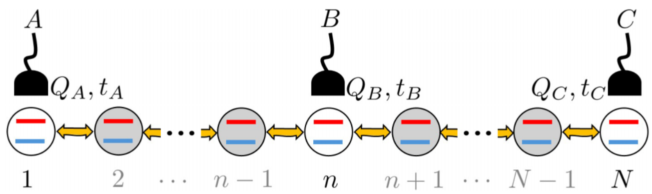

FIG. 1. Measurement setup of the spatial Leggett-Garg inequality. The three parties A, B, and C, displaced in space and connected by spin-1/2 chains, measure Q_A, Q_B, and Q_C at the respective times t_A, t_B, and t_C. In our implementation of the inequality we consider the spatiotemporally symmetric scenario $N = 2n - 1$, $t_A = 0$, $t_B = t$, and $t_C = 2t$.

Performing a spatial Leggett-Garg experiment will allow quantifying, in a platform-independent manner, the ability to generate and propagate spatiotemporal correlations in such implementations.

II. SPATIAL LEGGETT-GARG INEQUALITIES

The original formulation of the Leggett-Garg inequality considers an observer performing the binary measurement Q on a system at the three subsequent times: t_A, t_B, and t_C. Next, one introduces the two-times correlation functions $c_{X,Y} = \langle Q(t_X)Q(t_Y)\rangle = \sum_{\{q_X,q_Y\}=\pm 1} q_X q_Y P_{q_X q_Y}(Q, t_X, t_Y)$, with $P_{xy}(Q, t_X, t_Y)$ being the joint probabilities of measuring the dichotomic observable Q at time t_X and getting q_X, and again Q at time t_Y and getting q_Y. It can be shown that the quantity $K = c_{A,B} + c_{B,C} - c_{A,C}$ satisfies the Leggett-Garg inequality $-3 \leqslant K \leqslant 1$ for a system respecting the macrorealistic assumptions, namely, macrorealism *per se* (i.e., that the observable Q has a well-defined value at each time t), noninvasive measurability, and induction (i.e., the fact that the outcome of a measurement is not influenced by what will be measured at later times) [3]. The upper-bound value $K = 1$, in particular, can be derived by considering the combinations that the value of Q takes in the possible classical scenarios and evaluating the correlators [2].

The Leggett-Garg inequality is violated by quantum dynamics, as can be seen already in simple two-level single-particle systems. A clear example is a spin-1/2 initialized in the state $|+\rangle$, with $\sigma^x|+\rangle = |+\rangle$ and $\sigma^{x,y,z}$ the Pauli matrices, and evolving under the Hamiltonian $\hat{H} = -h\sigma^z/2$. For three σ^x measurements at times $t_A = 0$, $t_B = t$, and $t_C = 2t$, one obtains $K = 2\cos(ht) - \cos(2ht)$, which yields the maximal inequality violation $K = 3/2$ at times $t = \pi/(3h) + 2p\pi/h$ and $t = 5\pi/(3h) + 2p\pi/h$, where p is a generic integer [24].

Let us now consider a many-body system to conceptually extend the Leggett-Garg inequality in space. For concreteness, see Fig. 1, we analyze a one-dimensional spin chain made of N two-level systems. We consider the three observers A, B, and C, each one measuring the same observable at their respective chain sites 1, n, and N, respectively at times t_A, t_B, and t_C. For simplicity, we will analyze the spatially symmetric configuration corresponding to $N = 2n - 1$ and simply take $t_A = 0$, $t_B = t$, and $t_C = 2t$. Note that, in this way, $n - 1$ labels the lattice distance between the measuring parties: for $n = 1$ all parties coincide; then $n = 2$ corresponds to three adjacent parties, $n = 3$ corresponds to three parties with one spin in between, and so on. It is easy to generalize the above simplifications, as well as to relax the assumptions on the spatial dimension, boundary conditions, chain length, and number of levels.

To derive the spatial Leggett-Garg inequality, we delocalize the measurements in space and redefine the correlation functions as $C_{X,Y} = \langle Q_X(t_X)Q_Y(t_Y)\rangle$, which describes the sequential expectation value of measuring Q at site X and time t_X and later Q at site Y and time t_Y. We define the spatial extension of the Leggett-Garg inequality as

$$-3 \leqslant K_n := C_{1,n} + C_{n,2n-1} - C_{1,2n-1} \leqslant 1. \tag{1}$$

Let us now put Eq. (1) into context. For $n = 1$, it represents the ordinary LGI, reviewed above for a single spin and whose violation has been detected in several systems over the years (among all, quarks [20], qutrits [13], trapped ion qubits [19], and molecules [21]). The $n > 1$ extension adds intrinsically different features to this standard LGI scenario. First, since we consider a multipartite system rather than a single system, our inequality captures the correlation dynamics *within* the system parts. Second, the $n > 1$ violation would indicate the incompatibility with a macrorealistic model for the global many-body system. Third, the correlator Eq. (1) is easier to implement than other well established tools to diagnose quantum dynamics such as out-of-time-ordered correlations [50–52], which typically require reversing the system's dynamics. Finally, note that various experiments over the years have aimed to demonstrate macrorealism by protecting the system against classically invasive measurements using techniques ranging from quantum memories [53] to quantum nondemolition measurements [28], always remaining in the *single-system framework* akin to $n = 1$.

III. APPLICATIONS

Our formulation Eq. (1) does not rely on the calibration of the measurement setting Q, the time evolution, or the initial state. Let us however specify these choices to illustrate the quantum dynamics of K_n in a concrete setting. We consider a Heisenberg chain in a magnetic field with open boundaries:

$$H = \sum_{i=1}^{N-1} \left(J_x\sigma_i^x\sigma_{i+1}^x + J_y\sigma_i^y\sigma_{i+1}^y + J_z\sigma_i^z\sigma_{i+1}^z\right) - \frac{h}{2}\sum_{i=1}^{N}\sigma_i^z, \tag{2}$$

where J_x, J_y, J_z, and h are the coupling constants. We first consider the isotropic case $J_x = J_y = J_z := J$. As initial state, we take the product state $|\Psi\rangle = |+\rangle^{\otimes N}$. Finally, the quantum correlators involved in the inequality are then readily computed as $C_{X,Y} = \mathrm{Re}\{\langle\Psi|\, Q_X(t_X)Q_Y(t_Y)\,|\Psi\rangle\}$ [54], with $Q_X = \sigma_X^x$.

The value of K_n can be calculated analytically in the simple case of $J = 0$. In this case, the result does not depend on n since all spins evolve independently under the local Hamiltonian $\propto\sigma^z$ and thus rotate in the xy plane under the action of the external field h. If the parties respectively measure the observables σ_1^x, $\sigma_n^x(t)$, and $\sigma_{2n-1}^x(2t)$, where the lower index indicates the chain site of the measurement, we obtain $K_n = [3\cos(ht) - 2\cos(2ht) + \cos(3ht)]/2$ (see Appendix A). This function, depicted as the black solid line

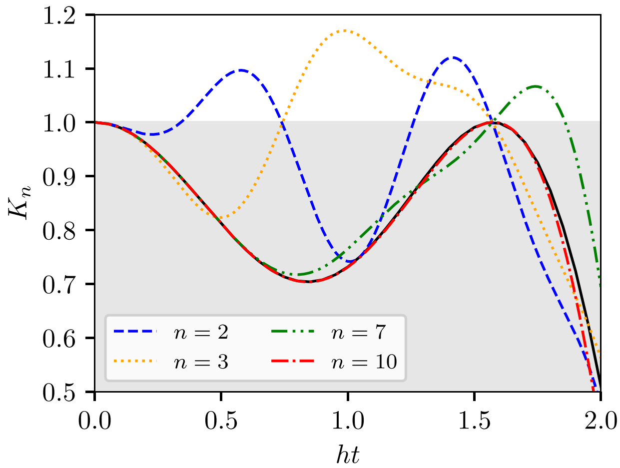

FIG. 2. Dynamics of the spatial Leggett-Garg inequality Eq. (1) in the spin chain Eq. (2) with $J = 1$ and $h = 1$ for various distances n between measuring parties and $Q = \sigma^x$. The black solid curve represents the noninteracting case of $J = 0$ and $h = 1$, in which no correlations can be established and the inequality is never violated. Note that violations are more difficult in longer chains, which tend to the noninteracting curve, and that the first violation time is ordered with n (see Fig. 3). Note that, for $n \geqslant 10$, the first violation time moves to the next period, i.e., the region around $ht \sim 2\pi$ of Fig. 5, where inequality violation revivals for $n < 10$ also occur.

in Fig. 2, does not lead to any inequality violation. This result suggests that, to observe LGI violations, the interactions between the spins are necessary. Indeed, for any noninteracting Hamiltonian one finds $[Q_X(t_X), Q_Y(t_Y)] = 0$ for $X \neq Y$ and $X, Y \in \{A, B, C\}$ and, under this assumption, only one can prove that the inequality Eq. (1) cannot be violated (see Appendix A). However, not all interacting evolutions might be detected by the inequality.

Let us now consider nonzero interactions and analyze the violations of the spatial LGI. We discuss the numerical results for the Hamiltonian (2), presented in Fig. 2 for the values of $J = 1$ and of $h = 1$. Setting $J \neq 0$ allows for violations of the inequality, which occur at times close to the maxima of the noninteracting black curve, which we are perturbing by considering $J > 0$. Also note that, as n increases, the short-time noninteracting profile is recovered for increasingly large time intervals. Thus the overall message of Fig. 2 is that, if there are violations for a certain initial state, Hamiltonian, and measurements, then increasing the length of the chain tends to increase the first violation time. This phenomenon is a consequence of the existence of a maximum velocity, the Lieb-Robinson bound [38], at which correlations can propagate in a spin chain. We actually note that the Lieb-Robinson bound can be exceeded (and the LGI inequality violated) by small correlations. However, since these are exponentially suppressed with the system size, our formalization can characterize the nonrelativistic correlation dynamics of the system quantitatively.

Additionally, for a given Hamiltonian and initial state, the measurements may be more or less optimal for observing a violation at a given time. To reduce this variability, we perform a measurement optimization to maximize the value of K_n at each time step [23]. The details of such optimization are discussed in Appendix B, where we indeed verify that the strength of the violation can be substantially increased with respect to the nonoptimized case (see Table I). Note that, as expected, the violation strength diminishes for long chains and tends to the noninteracting $J = 0$ curve, especially for short times.

TABLE I. Maximal value of the K_n correlator for times $ht \leqslant 1.8$ and the nearest-neighbor Hamiltonian Eq. (2) with $J = 1, h = 1$ (NN) and its next-nearest-neighbor (NNN) extension.

n	2	3	4	5	6	7
NN	1.381	1.351	1.197	1.236	1.024	1.160
NNN	1.391	1.244	1.285	1.248	1.024	1.206

We plot in Fig. 3(a) the optimized first-violation times $h\tau$ versus n, which further demonstrates the relation between the spatial LGI violation and the correlation dynamics. In particular, to detect the violation and define τ, we choose the conservative threshold $K_n \sim 1.02$ to be safely above the magnitude of the numerical errors and within the resolution of experiments [55]. Our method provides a rigorous upper bound of the Lieb-Robinson time for *each* system size n, or, equivalently, a lower bound on the Lieb-Robinson velocity.

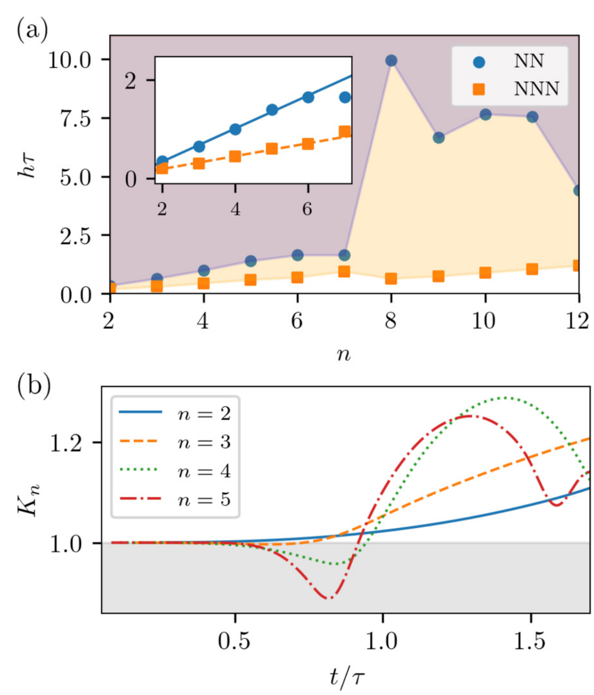

FIG. 3. (a) Time of the first inequality violation τ versus distance n (corresponding to $N = 2n - 1$ spins), showing that the speed of quantum correlations propagation in the spin chain is limited (we use the criterion $K_n > 1.02$ to determine τ). The points correspond to nearest-neighbor (NN) Hamiltonian Eq. (2) with $J = 1, h = 1$, while the squares correspond to its next-nearest-neighbor (NNN) extension (see text). The shaded regions exclude the Lieb Robinson time and, in the inset, the straight lines fit the points $2 \leqslant n \leqslant 6$ to simply emphasize their trend. (b) Optimized spatial Leggett-Garg correlator versus normalized time for the NNN case and various distances n.

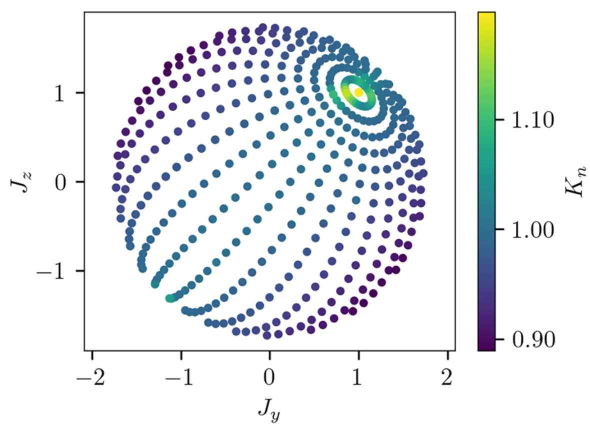

FIG. 4. Maximal violation of the spatial Leggett-Garg inequality up to time $ht = 2$, evaluated for the Hamiltonian Eq. (2) with $n = 4$ ($N = 7$). Here we optimize over the measurements Q, take the initial state $|+\rangle^{\otimes N}$, and set $J_x = \sqrt{3 - J_y^2 - J_z^2}$. The inequality violation is maximal for the Heisenberg model $J_x = J_y = J_z = 1$, under which correlations optimally spread. Note that the results remain invariant under reflection of all couplings, i.e., under $J_{x,y,z} \to -J_{x,y,z}$.

Note that, for nearest-neighbor model data (NN) corresponding to $n \geqslant 8$, the first violation time quickly increases because such violation occurs in the second period of the corresponding noninteracting model (cf. Fig. 5). Moreover, for small distances n, we observe a linear behavior between n and $h\tau$, see Fig. 3(a) inset and Fig. 3(b), which indicates that short-time correlations spread in a light-cone manner with constant velocity consistently with the Lieb-Robinson bounds.

To further confirm the connection between Lieb-Robinson physics and the inequality violation, we include in Fig. 3(a) next-nearest-neighbor (NNN) interactions in the Hamiltonian. In particular, by adding the term $J\sum_{i=1}^{N-2}\vec{\sigma}_i \cdot \vec{\sigma}_{i+2}$ to Eq. (2), with $\vec{\sigma}_i = (\sigma_i^x, \sigma_i^y, \sigma_i^z)^T$, we observe again a linear proportionality between τ and n, but the slope of the curve decreases [orange squares in Fig. 3(a)]. In other words, the spatial Leggett-Garg inequality violation is accelerated by enabling longer-range interactions that allow for a faster spreading of quantum correlations. Note that, for small system sizes, we actually obtain that the inequality is violated for any finite time $t > 0$. This may occur because the sites $1, n, 2n - 1$ are directly coupled through the extended Hamiltonian for $n = 2, 3$, while for $n > 3$ these sites do not interact directly and a finite time is needed to violate the LGI.

To gain further insight into which dynamics enable the violation of the spatial Leggett-Garg inequality, we consider the Hamiltonian (2) with the couplings constrained to $J_x^2 + J_y^2 + J_z^2 = 3$ [56] and plot in Fig. 4 the maximal violation. We observe that the strongest violation occurs for isotropic interactions, while only marginal violation is observed for the XXZ model ($J_y = J_z$). Indeed, we note that the single-particle term (with coupling h) produces the maximal violation of the single-site LGI in this setting. The isotropic interacting term, in turn, corresponds to a chain of nearest-neighbor SWAP operators and both terms commute. In the Heisenberg picture, the interacting term propagates operators along the chain so that, after sufficient time, they overlap. At that point, the single-particle term rotates the state, producing a notable violation in the multisite LGI. The fact that isotropic interactions are optimal also facilitates the LGI implementation in the experimental platforms, where large anisotropic couplings are feasible, but nonetheless more challenging to achieve than isotropic ones [57].

Interestingly, the violation of the spatial LGI in our setting indicates that the Hamiltonian is close to a Heisenberg chain, which could be useful for Hamiltonian learning and certification protocols [58,59]. Learning features of the Hamiltonian (for example, the couplings J_x, J_y, J_z) from experimental data alone is a highly resource intensive task and has been tackled with a plethora of methods [60–62], also experimentally [63]. Our inequality, which is only based on three correlators and does not require trust in the measurement settings, may provide an advantage in this task.

The protocol of our work can be implemented in the available experimental platforms [39–49]. For instance, ultracold atoms in optical lattices currently offer the possibility of preparing suitable initial states and performing a nonlocal time evolution with a prescribed Hamiltonian [64]. By equipping such experiments with single-site addressability, the spin state can be imaged at the prescribed times and sites and the measurement outcomes recorded. After enough rounds of collecting data, the statistics involved in LGI Eq. (2) (or in temporal Bell inequalities [65]) can be inferred.

Concerning the resilience of our results to environmental disturbance, we envision neutral atom devices [45] (e.g., quantum simulators) as suitable platforms for an experimental realization of our proposal. In these devices, especially optical tweezer arrays or Rydberg systems, the timescales T_1 and T_2 of lifetime and coherence respectively can reach values on the order of seconds or longer [66–68] and provide inherent scalability. As such, engineering first violation times being $\ll T_{1,2}$ (hence a field h of the order of $[0.1, 10]\ \mathrm{s}^{-1}$) would enable protection from these effects. In Appendix B, we analyze the effect of perturbed measurements on the violation, showing that it remains robust. Nonetheless, an in-depth theoretical study in this direction would represent a compelling continuation of the present work. This could be accompanied by modeling platform-dependent effects of disorder and losses that could further reduce the measurement contrast.

IV. CONCLUSIONS

In conclusion, we conceptually extend the Leggett-Garg inequality to analyze the correlation dynamics of a quantum many-body system. Our spatial Leggett-Garg inequality can be implemented on existing experimental platforms, providing a practical way to quantify their ability to induce spatiotemporal correlations. Moreover, it provides a rigorous lower bound on the Lieb-Robinson velocity in an agnostic way, namely without full knowledge of the underlying Hamiltonian. Also, investigating the extension of these results to 2D and 3D systems could reveal insights about the spreading of quantum correlations in more complex geometries. Finally, a natural direction for future research is to relate our construction to the twin problem of extending Bell inequalities to the temporal domain [54,65,69], potentially through frameworks that aim to unify the description of space and time in nonrelativistic quantum physics [70].

ACKNOWLEDGMENTS

We thank G. Rajchel-Mieldzioć and M. Płodzień for early discussions on the topic and N. Gisin, A. Aspect, and Č. Brukner for comments and discussions. G.M. and A.T. acknowledge financial support of the Horizon Europe programme HORIZON-CL4-2022-QUANTUM-02-SGA via Project No. 101113690 (PASQuanS2.1) and A.T. acknowledges funding by the European Union under the Horizon Europe MSCA programme via Project No. 101146753 (QUANTIFLAC). D.F. acknowledges financial support from PNRR MUR Project No. PE0000023-NQSTI. ICFO-QOT group acknowledges support from European Research Council AdG NOQIA; MCIN/AEI [Grants No. PGC2018-0910.13039/501100011033 and No. CEX2019-000910-S/10.13039/501100011033, Plan National STAMEENA PID2022-139099NB, project funded by MCIN and by the "European Union NextGenerationEU/PRTR" (PRTR-C17.I1), FPI]; QUANTERA DYNAMITE PCI2022-132919; QuantERA II Programme co-funded by European Union's Horizon 2020 program under Grant Agreement No. 101017733; Ministry for Digital Transformation and of Civil Service of the Spanish Government through the QUANTUM ENIA project call–Quantum Spain project, and by the European Union through the Recovery, Transformation and Resilience Plan–NextGenerationEU within the framework of the Digital Spain 2026 Agenda; Grant No. MICIU/AEI/10.13039/501100011033 and EU (No. PCI2025-163167); Fundació Cellex; Fundació Mir-Puig; Generalitat de Catalunya (European Social Fund FEDER and CERCA program); Barcelona Supercomputing Center MareNostrum (Grant No. FI-2023-3-0024); funded by the European Union (Grants No. HORIZON-CL4-2022-QUANTUM-02-SGA, No. PASQuanS2.1, No. 101113690, EU Horizon 2020 FET-OPEN OPTOlogic, Grant No. 899794, QU-ATTO, Grant No. 101168628), EU Horizon Europe Program (Grant No. 101080086 NeQST and Grant Agreement No. 101080086 NeQST).

DATA AVAILABILITY

The correlators are computed using exact diagonalization methods (for small n) and standard time-evolving block decimation (TEBD) and time-dependent variational principle (TDVP) for the NN and NNN cases, respectively, implemented in TeNPy. Codes and data to generate the figures can be found in [71].

APPENDIX A: NONINTERACTING HAMILTONIANS

Here we discuss the spatial LGI for noninteracting Hamiltonians, i.e., for those containing only local couplings. To begin with, we consider the noninteracting version of Eq. (2), i.e., $H = -(h/2)\sum_i \sigma_i^z$, and derive the dynamics of K_n for the measurement $Q = \sigma^x$ and the state $|\Psi\rangle$. Elementary calculations show that $C_{1,n} = \cos(ht)$, $C_{n,2n} = \cos(ht)\cos(2ht)$, and $C_{1,2n-1} = \cos(2ht)$, which add up to $K_n = [3\cos(ht) - 2\cos(2ht) + \cos(3ht)]/2$. This quantity, depicted as the black solid line of Fig. 5, does not violate the LGI. The result of Fig. 5 prompts us to consider interactions to change the $J = 0$ curve and observe violation of the spatial Leggett-Garg inequality (cf. Fig. 6 in this Appendix). Indeed, interactions couple the spins which dynamically become nonseparable. Roughly speaking, time evolution brings the state of the spin chain closer to the one of a single quantum system, which violates the inequality (see, for instance, the blue dashed curve in Fig. 5) [72,73].

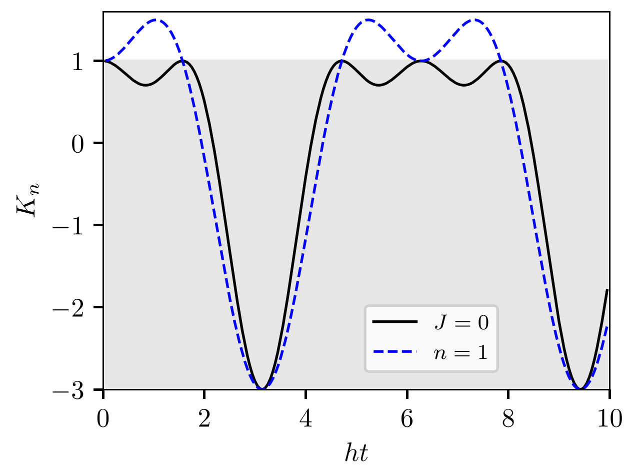

FIG. 5. Comparison of the Leggett-Garg dynamics for a single spin $n = 1$ and its spatial extension for noninteracting Hamiltonian $J = 0$ for any $n > 1$ and observable $Q = \sigma^x$.

More generally, we can prove that, under evolution governed by noninteracting Hamiltonians, the spatial LGI cannot be violated. Indeed, for noninteracting evolution, the observables $(Q_1(0), Q_n(t), Q_{2n-1}(2t))$ commute pairwise, as it happens for $t = 0$. Thus they are jointly measurable with outcomes $(q_1, q_n, q_{2n-1}) \in \{\pm 1\}$ with probability $p(q_1, q_n, q_{2n-1})$ (which depends on $|\Psi\rangle$). Thus the value

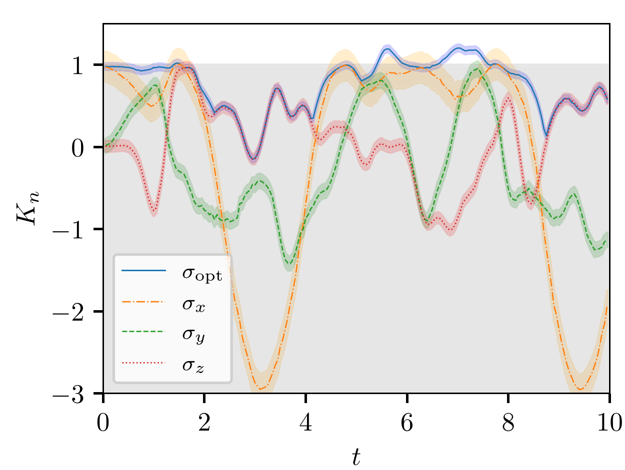

FIG. 6. Average dynamics of the Leggett-Garg correlator for measurement settings Q for $Q^{\rm ideal} = \sigma^x, \sigma^y, \sigma^z$ and noise level $\epsilon = 0.1$ for $n = 5$. We also display the data for the best setting $Q^{\rm ideal} = \sigma^{\rm opt}$ optimized at each time instance and subject to the same noise level $\epsilon = 0.1$.

of the correlator is $K_n = \sum_{q_1,q_n,q_{2n-1}} p(q_1, q_n, q_{2n-1})(q_1 q_n + q_n q_{2n-1} - q_1 q_{2n-1})$. By convexity, the maximal of K_N is attained by a deterministic strategy $p(q_1, q_n, q_{2n-1}) = \delta_{q_1,a}\delta_{q_2,b}\delta_{q_3,c}$, with δ the Kronecker's delta. Simple enumeration of all the values of K_n for $(a, b, c) \in \{\pm 1\}$ verifies that K_n is confined between -3 and 1. Note that the claim holds regardless the initial state $|\Psi\rangle$ (separable or entangled) and the details of the local measurement Q.

APPENDIX B: OPTIMIZATION OVER MEASUREMENTS

In this Appendix, we detail the procedure to optimize the correlator over measurements. Specifically, we find the measurement orientation $\vec{v} \in \mathbb{S}^2$, $\sigma^v = \vec{v} \cdot \vec{\sigma}$, such that K_n is maximal. To that end, we evaluate K_n for $Q = \sigma^v$, obtaining $K_n(\vec{v}) = \vec{v}^T \mathcal{K}_n \vec{v}$, where $\mathcal{K}_n$ is a 3×3 symmetric matrix with elements $[\mathcal{K}]_{pq} = \mathrm{Re}\{\langle\Psi|\hat{\mathcal{K}}_{pq}|\Psi\rangle\}$, with $p, q \in \{x, y, z\}$ and $\hat{\mathcal{K}}_{pq} = \sigma_1^p(0)\sigma_n^q(n) + \sigma_n^p(n)\sigma_{2n-1}^q(2n) - \sigma_1^p(0)\sigma_{2n-1}^q(2n)$. From the bilinear structure of the correlator, it is direct to see that $K_n(\vec{v}) \leqslant \lambda_{\max}(\mathcal{K}_n) = K_n(\vec{v}_{\max})$, where $\lambda_{\max}$ denotes the maximal eigenvalue and $\vec{v}_{\max}$ the corresponding eigenvector (the optimal measurement is $\sigma^{\mathrm{opt}} = \vec{v}_{\max} \cdot \vec{\sigma}$). In Fig. 6 we display an example of such optimization for distance $n = 5$ in the presence of noise disturbing the measurement settings. To that end, we perturb the ideal setting with Gaussian noise $Q \propto Q^{\mathrm{ideal}} + \epsilon \mathbf{n} \cdot \boldsymbol{\sigma}$, where $\mathbf{n} = (n^x, n^y, n^z)$ are samples dependent of the normal distribution. We display the average and fluctuations of the dynamics of the Leggett-Garg correlator over various samples.

Note that, from an experimental perspective, the evaluation of the maximal nonlocality requires the inference of the matrix $\mathcal{K}$ involving sequential expectation values of the form $\langle\sigma_i^p(t_i)\sigma_j^q(t_j)\rangle$ for all spin components $p, q \in \{x, y, z\}$. We also observe that the violation is robust against noise and that different observables are affected differently; for example, σ_x is more sensitive to noise than σ_y and σ_z. We leave the optimization of the measurements, taking noise into account, for future studies.

Next, in Table I, we specify the maximal violation for short times, which suggests that extended Hamiltonians not only accelerate the onset of violation but also strengthen its magnitude.

[1] A. J. Leggett and A. Garg, Quantum mechanics versus macroscopic realism: Is the flux there when nobody looks? Phys. Rev. Lett. **54**, 857 (1985).

[2] C. Emary, N. Lambert, and F. Nori, Leggett–Garg inequalities, Rep. Prog. Phys. **77**, 016001 (2014).

[3] G. Vitagliano and C. Budroni, Leggett-Garg macrorealism and temporal correlations, Phys. Rev. A **107**, 040101 (2023).

[4] A. Palacios-Laloy, F. Mallet, F. Nguyen, P. Bertet, D. Vion, D. Esteve, and A. N. Korotkov, Experimental violation of a Bell's inequality in time with weak measurement, Nat. Phys. **6**, 442 (2010).

[5] M. E. Goggin, M. P. Almeida, M. Barbieri, B. P. Lanyon, J. L. O'Brien, A. G. White, and G. J. Pryde, Violation of the Leggett–Garg inequality with weak measurements of photons, Proc. Natl. Acad. Sci. USA **108**, 1256 (2011).

[6] J. Dressel, C. J. Broadbent, J. C. Howell, and A. N. Jordan, Experimental violation of two-party Leggett-Garg inequalities with semiweak measurements, Phys. Rev. Lett. **106**, 040402 (2011).

[7] V. Athalye, S. S. Roy, and T. S. Mahesh, Investigation of the Leggett-Garg inequality for precessing nuclear spins, Phys. Rev. Lett. **107**, 130402 (2011).

[8] G. C. Knee, S. Simmons, E. M. Gauger, J. J. Morton, H. Riemann, N. V. Abrosimov, P. Becker, H. Pohl, K. M. Itoh, M. L. Thewalt, *et al.*, Violation of a Leggett–Garg inequality with ideal non-invasive measurements, Nat. Commun. **3**, 606 (2012).

[9] Z.-Q. Zhou, S. F. Huelga, C.-F. Li, and G.-C. Guo, Experimental detection of quantum coherent evolution through the violation of Leggett-Garg-type inequalities, Phys. Rev. Lett. **115**, 113002 (2015).

[10] J. A. Formaggio, D. I. Kaiser, M. M. Murskyj, and T. E. Weiss, Violation of the Leggett-Garg inequality in neutrino oscillations, Phys. Rev. Lett. **117**, 050402 (2016).

[11] G. C. Knee, K. Kakuyanagi, M.-C. Yeh, Y. Matsuzaki, H. Toida, H. Yamaguchi, S. Saito, A. J. Leggett, and W. J. Munro, A strict experimental test of macroscopic realism in a superconducting flux qubit, Nat. Commun. **7**, 13253 (2016).

[12] H. Katiyar, A. Brodutch, D. Lu, and R. Laflamme, Experimental violation of the Leggett–Garg inequality in a three-level system, New J. Phys. **19**, 023033 (2017).

[13] K. Wang, C. Emary, X. Zhan, Z. Bian, J. Li, and P. Xue, Enhanced violations of Leggett-Garg inequalities in an experimental three-level system, Opt. Express **25**, 31462 (2017).

[14] X. Liu, Z.-Q. Zhou, Y.-J. Han, Z.-F. Li, J. Hu, T.-S. Yang, P.-Y. Li, C. Liu, X. Li, Y. Ma, P.-J. Liang, C.-F. Li, and G.-C. Guo, Strict experimental test of macroscopic realism in a light-matter-interfaced system, Phys. Rev. A **100**, 032106 (2019).

[15] K. Wang, M. Xu, L. Xiao, and P. Xue, Experimental violations of Leggett-Garg inequalities up to the algebraic maximum for a photonic qubit, Phys. Rev. A **102**, 022214 (2020).

[16] A. Santini and V. Vitale, Experimental violations of Leggett-Garg inequalities on a quantum computer, Phys. Rev. A **105**, 032610 (2022).

[17] T. Zhan, C. Wu, M. Zhang, Q. Qin, X. Yang, H. Hu, W. Su, J. Zhang, T. Chen, Y. Xie, W. Wu, and P. Chen, Experimental violation of the Leggett-Garg inequality in a three-level trapped-ion system, Phys. Rev. A **107**, 012424 (2023).

[18] E. Kreuzgruber, R. Wagner, N. Geerits, H. Lemmel, and S. Sponar, Violation of a Leggett-Garg inequality using ideal negative measurements in neutron interferometry, Phys. Rev. Lett. **132**, 260201 (2024).

[19] P. Lu, X. Rao, T. Liu, Y. Liu, J. Bian, F. Zhu, and L. Luo, Experimental demonstration of enhanced violations of Leggett-Garg inequalities in asymmetric trapped-ion qubit, Phys. Rev. A **109**, 042205 (2024).

[20] K. Cheng and B. Yan, Bell inequality violation of light quarks in dihadron pair production at lepton colliders, Phys. Rev. Lett. **135**, 011902 (2025).

[21] A. Chatterjee, H. Karthik, T. Mahesh, and A. Usha Devi, Extreme violations of Leggett-Garg inequalities for a system evolving under superposition of unitaries, Phys. Rev. Lett. **135**, 220202 (2025).
[22] D. Avis, P. Hayden, and M. M. Wilde, Leggett-Garg inequalities and the geometry of the cut polytope, Phys. Rev. A **82**, 030102(R) (2010).
[23] C. Budroni, T. Moroder, M. Kleinmann, and O. Gühne, Bounding temporal quantum correlations, Phys. Rev. Lett. **111**, 020403 (2013).
[24] J. Kofler and Č. Brukner, Conditions for quantum violation of macroscopic realism, Phys. Rev. Lett. **101**, 090403 (2008).
[25] J. Naikoo, A. K. Alok, S. Banerjee, and S. U. Sankar, Leggett-Garg inequality in the context of three flavor neutrino oscillation, Phys. Rev. D **99**, 095001 (2019).
[26] M. Blasone, F. Illuminati, L. Petruzziello, and L. Smaldone, Leggett-Garg inequalities in the quantum field theory of neutrino oscillations, Phys. Rev. A **108**, 032210 (2023).
[27] M. M. Wilde and A. Mizel, Addressing the clumsiness loophole in a Leggett-Garg test of macrorealism, Found. Phys. **42**, 256 (2012).
[28] C. Budroni, G. Vitagliano, G. Colangelo, R. J. Sewell, O. Gühne, G. Tóth, and M. W. Mitchell, Quantum nondemolition measurement enables macroscopic Leggett-Garg tests, Phys. Rev. Lett. **115**, 200403 (2015).
[29] S. Majidy, J. J. Halliwell, and R. Laflamme, Detecting violations of macrorealism when the original Leggett-Garg inequalities are satisfied, Phys. Rev. A **103**, 062212 (2021).
[30] J. J. Halliwell, Comparing conditions for macrorealism: Leggett-Garg inequalities versus no-signaling in time, Phys. Rev. A **96**, 012121 (2017).
[31] F. J. Gómez-Ruiz, J. J. Mendoza-Arenas, F. J. Rodríguez, C. Tejedor, and L. Quiroga, Quantum phase transitions detected by a local probe using time correlations and violations of Leggett-Garg inequalities, Phys. Rev. B **93**, 035441 (2016).
[32] J. Mendoza-Arenas, F. Gómez-Ruiz, F. Rodríguez, and L. Quiroga, Enhancing violations of Leggett-Garg inequalities in nonequilibrium correlated many-body systems by interactions and decoherence, Sci. Rep. **9**, 17772 (2019).
[33] T. S. Cubitt and J. I. Cirac, Engineering correlation and entanglement dynamics in spin systems, Phys. Rev. Lett. **100**, 180406 (2008).
[34] M. Cheneau, P. Barmettler, D. Poletti, M. Endres, P. Schauß, T. Fukuhara, C. Gross, I. Bloch, C. Kollath, and S. Kuhr, Light-cone-like spreading of correlations in a quantum many-body system, Nature (London) **481**, 484 (2012).
[35] L. Bonnes, F. H. Essler, and A. M. Läuchli, "light-cone" dynamics after quantum quenches in spin chains, Phys. Rev. Lett. **113**, 187203 (2014).
[36] M. C. Arnesen, S. Bose, and V. Vedral, Natural thermal and magnetic entanglement in the 1D Heisenberg model, Phys. Rev. Lett. **87**, 017901 (2001).
[37] L. Amico, R. Fazio, A. Osterloh, and V. Vedral, Entanglement in many-body systems, Rev. Mod. Phys. **80**, 517 (2008).
[38] E. H. Lieb and D. W. Robinson, The finite group velocity of quantum spin systems, Commun. Math. Phys. **28**, 251 (1972).
[39] A. Browaeys and T. Lahaye, Many-body physics with individually controlled Rydberg atoms, Nat. Phys. **16**, 132 (2020).
[40] P. Scholl, H. J. Williams, G. Bornet, F. Wallner, D. Barredo, L. Henriet, A. Signoles, C. Hainaut, T. Franz, S. Geier, A. Tebben, A. Salzinger, G. Zürn, T. Lahaye, M. Weidemüller, and A. Browaeys, Microwave engineering of programmable XXZ Hamiltonians in arrays of Rydberg atoms, PRX Quantum **3**, 020303 (2022).
[41] S. Geier, N. Thaicharoen, C. Hainaut, T. Franz, A. Salzinger, A. Tebben, D. Grimshandl, G. Zürn, and M. Weidemüller, Floquet Hamiltonian engineering of an isolated many-body spin system, Science **374**, 1149 (2021).
[42] C. Miller, A. N. Carroll, J. Lin, H. Hirzler, H. Gao, H. Zhou, M. D. Lukin, and J. Ye, Two-axis twisting using Floquet-engineered XYZ spin models with polar molecules, Nature (London) **633**, 332 (2024).
[43] I. Bloch, J. Dalibard, and S. Nascimbene, Quantum simulations with ultracold quantum gases, Nat. Phys. **8**, 267 (2012).
[44] C. Gross and I. Bloch, Quantum simulations with ultracold atoms in optical lattices, Science **357**, 995 (2017).
[45] D. Wei, A. Rubio-Abadal, B. Ye, F. Machado, J. Kemp, K. Srakaew, S. Hollerith, J. Rui, S. Gopalakrishnan, N. Y. Yao, I. Bloch, and J. Zeiher, Quantum gas microscopy of Kardar-Parisi-Zhang superdiffusion, Science **376**, 716 (2022).
[46] R. Blatt and C. F. Roos, Quantum simulations with trapped ions, Nat. Phys. **8**, 277 (2012).
[47] C. Monroe, W. C. Campbell, L.-M. Duan, Z.-X. Gong, A. V. Gorshkov, P. W. Hess, R. Islam, K. Kim, N. M. Linke, G. Pagano, P. Richerme, C. Senko, and N. Y. Yao, Programmable quantum simulations of spin systems with trapped ions, Rev. Mod. Phys. **93**, 025001 (2021).
[48] P. N. Jepsen, J. Amato-Grill, I. Dimitrova, W. W. Ho, E. Demler, and W. Ketterle, Spin transport in a tunable Heisenberg model realized with ultracold atoms, Nature (London) **588**, 403 (2020).
[49] A. Signoles, T. Franz, R. Ferracini Alves, M. Gärttner, S. Whitlock, G. Zürn, and M. Weidemüller, Glassy dynamics in a disordered Heisenberg quantum spin system, Phys. Rev. X **11**, 011011 (2021).
[50] I. Garça-Mata, R. Jalabert, and D. Wisniacki, Out-of-time-order correlations and quantum chaos, Scholarpedia **18**, 55237 (2023).
[51] C.-J. Lin and O. I. Motrunich, Out-of-time-ordered correlators in a quantum Ising chain, Phys. Rev. B **97**, 144304 (2018).
[52] J. Riddell and E. S. Sørensen, Out-of-time ordered correlators and entanglement growth in the random-field XX spin chain, Phys. Rev. B **99**, 054205 (2019).
[53] J. P. Paz and G. Mahler, Proposed test for temporal Bell inequalities, Phys. Rev. Lett. **71**, 3235 (1993).
[54] T. Fritz, Quantum correlations in the temporal Clauser–Horne–Shimony–Holt (CHSH) scenario, New J. Phys. **12**, 083055 (2010).
[55] With ultracold atoms, correlators analogous to $C_{X,Y}$ are only measured with a few percent accuracy at most [34].
[56] Since the inequality violation occurs after the Lieb-Robinson time, and the Lieb-Robinson velocity roughly scales with J [65], this spherical constraint enables a fair comparison between the Hamiltonians (2).
[57] K. Kim, F. Yang, K. Mølmer, and J. Ahn, Realization of an extremely anisotropic Heisenberg magnet in Rydberg atom arrays, Phys. Rev. X **14**, 011025 (2024).

[58] J. Zhang and M. Sarovar, Quantum Hamiltonian identification from measurement time traces, Phys. Rev. Lett. **113**, 080401 (2014).

[59] N. Wiebe, C. Granade, C. Ferrie, and D. G. Cory, Hamiltonian learning and certification using quantum resources, Phys. Rev. Lett. **112**, 190501 (2014).

[60] W. Yu, J. Sun, Z. Han, and X. Yuan, Robust and efficient Hamiltonian learning, Quantum **7**, 1045 (2023).

[61] F. Wilde, A. Kshetrimayum, I. Roth, D. Hangleiter, R. Sweke, and J. Eisert, Scalably learning quantum many-body Hamiltonians from dynamical data, Quantum Sci. Technol. **11**, 035002 (2026).

[62] A. Gu, L. Cincio, and P. J. Coles, Practical Hamiltonian learning with unitary dynamics and Gibbs states, Nat. Commun. **15**, 312 (2024).

[63] S.-A. Guo, Y.-K. Wu, J. Ye, L. Zhang, Y. Wang, W.-Q. Lian, R. Yao, Y.-L. Xu, C. Zhang, Y.-Z. Xu, B.-X. Qi, P.-Y. Hou, L. He, Z.-C. Zhou, and L.-M. Duan, Hamiltonian learning for 300 trapped ion qubits with long-range couplings, Sci. Adv. **11**, eadt4713 (2025).

[64] Z. Zhu, Y. Kiefer, S. Jele, M. Gächter, G. Bisson, K. Viebahn, and T. Esslinger, Splitting and connecting singlets in atomic quantum circuits, Phys. Rev. X **15**, 041032 (2025).

[65] A. Tononi and M. Lewenstein, Temporal Bell inequalities in non-relativistic many-body physics, Quantum Sci. Technol. **10**, 03LT01 (2025).

[66] M. Saffman, Quantum computing with atomic qubits and Rydberg interactions: Progress and challenges, J. Phys. B **49**, 202001 (2016).

[67] T. M. Graham, Y. Song, J. Scott, C. Poole, L. Phuttitarn, K. Jooya, P. Eichler, X. Jiang, A. Marra, B. Grinkemeyer, *et al.*, Multi-qubit entanglement and algorithms on a neutral-atom quantum computer, Nature (London) **604**, 457 (2022).

[68] J. P. Covey, H. Weinfurter, and H. Bernien, Quantum networks with neutral atom processing nodes, npj Quantum Inf. **9**, 90 (2023).

[69] J. Dressel and A. N. Korotkov, Avoiding loopholes with hybrid Bell-Leggett-Garg inequalities, Phys. Rev. A **89**, 012125 (2014).

[70] F. Costa, M. Ringbauer, M. E. Goggin, A. G. White, and A. Fedrizzi, Unifying framework for spatial and temporal quantum correlations, Phys. Rev. A **98**, 012328 (2018).

[71] G. Müller-Rigat, Spatial-Leggett-Garg, Github repository, 2025, https://github.com/GuillemMRR/Spatial-Leggett-Garg.

[72] J. Watrous, *The Theory of Quantum Information* (Cambridge University Press, Cambridge, UK, 2018).

[73] This aligns with Naimark's dilation theorem, according to which (applied to our case) a operator-valued measure (POVM) on a given spin can be implemented through a projective measurement on another ancillary spin that has previously interacted with it [72].